© 2015. Published by The Company of Biologists Ltd | Journal of Cell Science (2015) 128, 3769-3780 doi:10.1242/jcs.173179

RESEARCH ARTICLE

Loss of protein phosphatase 6 in oocytes causes failure of meiosis II exit and impaired female fertility

Meng-Wen Hu[1,2,*], Zhen-Bo Wang[1,*], Yan Teng[3,*], Zong-Zhe Jiang[1,2], Xue-Shan Ma[1], Ning Hou[3], Xuan Cheng[3], Heide Schatten[4], Xingzhi Xu[5,‡], Xiao Yang[3,‡] and Qing-Yuan Sun[1,‡]

ABSTRACT

Dynamic protein phosphorylation and dephosphorylation, mediated by a conserved cohort of protein kinases and phosphatases, regulate cell cycle progression. Among the well-known PP2A-like protein phosphatases, protein phosphatase 6 (PP6) has been analyzed in mammalian mitosis, and Aurora A has recently been identified as its key substrate. However, the functions of PP6 in meiosis are still entirely unknown. To identify the physiological role of PP6 in female gametogenesis, *Ppp6c*$^{F/F}$ mice were first generated and crossed with *Zp3-Cre* mice to selectively disrupt *Ppp6c* expression in oocytes. Here, we report for the first time that PP6c is dispensable for oocyte meiotic maturation but essential for exit from meiosis II (MII) after fertilization. Depletion of PP6c caused an abnormal MII spindle and disrupted MII cytokinesis, resulting in zygotes with high risk of aneuploidy and defective early embryonic development, and thus severe subfertility. We also reveal that PP6 inactivation interferes with MII spindle formation and MII exit owing to increased Aurora A activity, and that Aurora A inhibition with MLN8237 can rescue the PP6c depletion phenotype. In conclusion, our findings uncover a hitherto unknown role for PP6 as an indispensable regulator of oocyte meiosis and female fertility.

KEY WORDS: Conditional knockout, PP6, Aurora A, Oocyte, MII exit, Aneuploidy

INTRODUCTION

In mammals, it is generally accepted that females are born with a finite number of oocytes contained within primordial follicles. In order to produce mature eggs, dormant primordial follicles are activated and subsequently develop into primary follicles, secondary follicles and antral follicles (Oktem and Urman, 2010). Throughout this follicular growth process, oocytes are all arrested at prophase of meiosis I (MI) with homologs held together by chiasmata, and they only grow in size (commonly referred to as the germinal vesicle stage). Finally, dominant antral follicles reach the pre-ovulatory stage and release the mature egg for fertilization after a gonadotropin surge (Hirshfield, 1991). Upon receiving ovulatory signals, these fully-grown, meiotically competent oocytes contained within preovulatory follicles resume meiosis, as indicated by germinal vesicle breakdown (GVBD), followed by spindle organization and chromosome alignment for coordinated chromosome segregation (Sun et al., 2009). After the first polar body extrusion (PBE), the oocytes are arrested at metaphase of meiosis II (MII) until being fertilized by sperm. The second meiosis is resumed and the second polar body is extruded upon fertilization (Jones, 2005; Mehlmann, 2005). Thus, a single haploid egg is generated through two consecutive chromosome segregations with only one round of DNA replication from one original diploid germ cell. Aneuploidy can occur in both meioses if chromosomes fail to segregate accurately, which is the leading genetic cause of infertility, pregnancy loss and many developmental disabilities (Hassold and Hunt, 2001).

During meiosis in oocytes, there are dynamic waves of protein phosphorylation and dephosphorylation, which regulate meiotic cell cycle arrest and progression, chromosome dynamics, and meiotic spindle assembly and disassembly (Schindler, 2011). Many of these phosphorylation and dephosphorylation events are mediated by a conserved cohort of protein kinases and phosphatases. The mouse genome encodes 561 protein kinases compared to only 162 protein phosphatases (Caenepeel et al., 2004). Historically, many studies focused on protein kinases, resulting in comparatively less information about the roles of protein phosphatases. Serine/threonine phosphoprotein phosphatases (PPPs), a major protein phosphatase family, have been implicated in regulating oocyte meiosis. Within the PPP family, the catalytic subunits of PP2A, PP4 and PP6 are most closely related, and the three proteins form a subfamily called PP2A-like protein phosphatases that account for the majority of cellular serine/threonine phosphatase activity (Janssens and Goris, 2001; Moorhead et al., 2007). PP2A is involved in regulating chromosome condensation, DNA damage repair, the G2/M transition and sister chromatid cohesion (Ruediger et al., 2011). We have recently shown that PP2A is essential for female meiosis and fertility because oocyte-specific depletion of PP2A facilitates GVBD, causes elongated MII spindles and precocious separation of sister chromatids, resulting in defective early embryonic development, and thus subfertility (Hu et al., 2014). Although having a high similarity with PP2A, PP6 has not had the same level of scientific examination, and its functions in meiosis still remain unknown.

The PP6 holoenzyme consists of a catalytic subunit, PP6c (also known as PPP6C), one of the three regulatory subunits including SAPS1, SAPS2 and SAPS3 (also known as PPP6R1, PPP6R2 and PPP6R3, respectively), and one of the three ankyrin repeat subunits including ARS-A, ARS-B and ARS-C (also known as ANKRD28, ANKRD44 and ANKRD52, respectively) (Stefansson and Brautigan, 2006; Stefansson et al., 2008). PP6 is conserved among all eukaryotic species from yeast to humans, attesting to

[1]State Key Laboratory of Reproductive Biology, Institute of Zoology, Chinese Academy of Sciences, Beijing 100101, China. [2]University of Chinese Academy of Sciences, Beijing 100101, China. [3]State Key Laboratory of Proteomics, Genetic Laboratory of Development and Disease, Institute of Biotechnology, 20 Dongdajie, Beijing 100071, China. [4]Department of Veterinary Pathobiology, University of Missouri, Columbia, MO 65211, USA. [5]Beijing Key Laboratory of DNA Damage Response and College of Life Sciences, Capital Normal University, Beijing 100048, China.
*These authors contributed equally to this work

‡Authors for correspondence (Xingzhi_Xu@mail.cnu.edu.cn; yangx@bmi.ac.cn; sunqy@ioz.ac.cn)

Received 16 April 2015; Accepted 3 September 2015

Journal of Cell Science (2015) 128, 3769-3780 doi:10.1242/jcs.173179

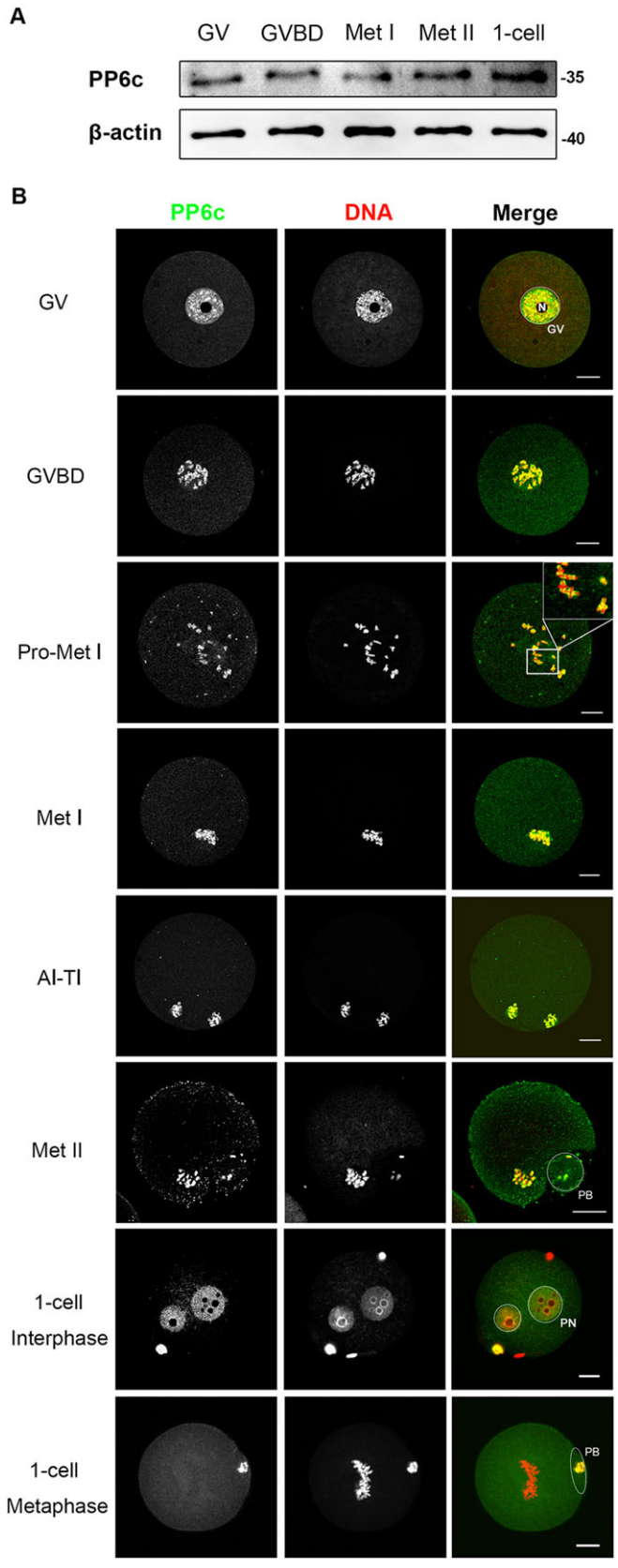

Fig. 1. Characterization of PP6c during mouse oocyte meiotic maturation. (A) Western blots showing the expression pattern of PP6c at different stages of oocytes and zygotes. A total of 200 oocytes were collected after being cultured for 0, 4, 8 and 13 h, corresponding to the germinal vesicle (GV), GVBD, metaphase of MI (Met I) and metaphase of MII (Met II) stages, respectively. A total of 200 one-cell embryos were collected at 26–28 h after hCG treatment with successful mating. Samples were immunoblotted using anti-PP6c and anti-β-actin antibodies. Molecular mass is given in kDa. (B) Representative images of subcellular localization of PP6c during oocyte meiotic maturation and after fertilization. Oocytes were double stained for PP6c (green) and DNA (red) at germinal vesicle (GV), GVBD, pro-metaphase I (Pro-Met I), Met I, anaphase I to telophase I (AI–TI) and Met II stages; one-cell embryos were double stained for PP6c (green) and DNA (red) at interphase and metaphase stages of the first mitotic division. A magnification of the boxed region is shown on the top right corner for the Pro-MI image. N, nucleolus; PN, pronuclei; PB, polar body. Scale bars: 20 µm.

its fundamental importance. Recently, it has been found that mutations in PP6c exist in 9–12.4% melanomas surveyed and might act as drivers for melanoma development (Hodis et al., 2012; Krauthammer et al., 2012). Sit4, the homolog in yeast, is required for G1/S progression and equal chromosome segregation in yeast (Sutton et al., 1991). The human PP6 has been shown to play a role in DNA damage response, cell cycle, apoptosis and pre-mRNA splicing by acting on DNA-dependent protein kinase (DNA-PK), histone γ-H2AX, Aurora A, NF-κB and the U1 small nuclear ribonucleic protein (snRNP) (Douglas et al., 2014, 2010; Hammond et al., 2013; Hosing et al., 2012; Kajihara et al., 2014; Kamoun et al., 2013; Stefansson and Brautigan, 2006, 2007; Zeng et al., 2010; Zhong et al., 2011). However, the role of PP6 in reproductive cells remains unclear.

Genetically modified mouse models are powerful tools for studying gene function *in vivo* (Hu et al., 2012; Sun et al., 2008). Here, we first generated $Ppp6c^{F/F}$ mice in which exons II–IV of the *Ppp6c* gene were flanked with *loxp* sites, and then used conditional knockout technology by crossing $Ppp6c^{F/F}$ mice with *Zp3-Cre* mice (Wang et al., 2013) to generate mutant mice with specific deletion of *Ppp6c* in oocytes from the primary follicle stage onwards, in order to investigate the function of PP6 in female meiosis and fertility within ovarian follicles *in vivo*. For the first time, we report that PP6 mutation causes female subfertility by disrupting MII spindle organization and MII exit after fertilization, without affecting follicle growth, ovulation or oocyte meiotic maturation.

RESULTS

Expression and subcellular localization of PP6 during oocyte maturation

To study the functions of PP6 in female meiosis, its expression was first analyzed by immunoblotting extracts from germinal vesicle oocytes to one-cell stage embryos using an antibody directed against human PP6c (Fig. 1A). The expression of PP6c throughout oocyte meiotic maturation did not show evident changes, with only a little upregulation after the metaphase of MI (metaphase-I) stage. The subcellular localization of PP6 was then examined by immunofluorescence staining (Fig. 1B). During oocyte maturation, the localization of PP6c was basically consistent at different stages. At the germinal vesicle stage, PP6c was concentrated in the germinal vesicle exhibiting strong punctate staining around the nucleolus. From the GVBD to metaphase of MII (metaphase-II) stage, PP6c was always localized to the chromosomes. In particular, PP6c accumulated strongly along the outer chromosome arms when all homologous chromosomes formed bivalents during the metaphase-I stage. In one-cell stage embryos, PP6c was concentrated in the pronuclei during interphase, but the protein lost its chromatin localization and dispersed into the cytoplasm when the embryos entered the first mitotic division. This specific localization of PP6c in oocytes

Journal of Cell Science (2015) 128, 3769-3780 doi:10.1242/jcs.173179

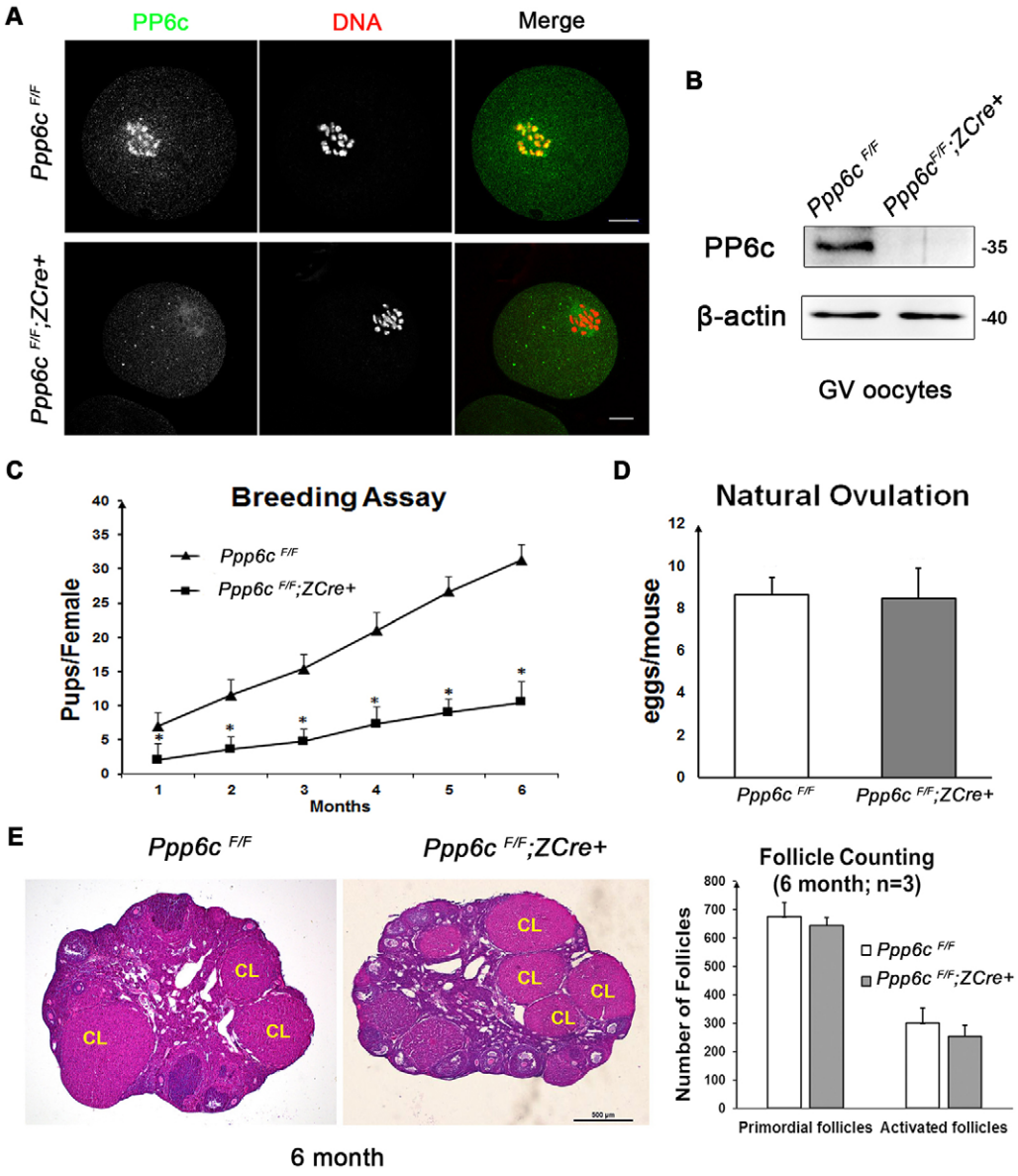

Fig. 2. Disruption of *Ppp6c* in oocytes leads to female subfertility without impacting ovulation. (A) Localization of PP6c in *Ppp6c*$^{F/F}$ and *Ppp6*$^{F/F}$*;ZCre+* oocytes. Germinal vesicle (GV) oocytes were cultured for about 4 h and those that had undergone GVBD were fixed, and subjected to immunofluorescence staining for PP6c (green) and DNA (red). Scale bars: 20 µm. All of the experiments were repeated at least three times, and representative results are shown. (B) Western blots showing the absence of PP6c protein expression in *Ppp6c*$^{F/F}$*;ZCre+* oocytes. Lysate from 200 germinal vesicle oocytes was loaded in each lane. Levels of β-actin were used as internal controls. Molecular mass is given in kDa. All of the experiments were repeated at least three times, and representative results are shown. (C) Subfertility of the female *Ppp6c*$^{F/F}$*;ZCre+* mice. Continuous breeding assessment showing the cumulative number of progeny per female mouse for 6 months. Results are mean±s.e.m., at least six mice of each genotype were used. (D) Normal ovulation rate in *Ppp6c*$^{F/F}$*;ZCre+* mice (mean±s.e.m.). Fertilized eggs were collected and counted from female mice of each genotype with vaginal plugs after mating overnight. At least 6 mice of each genotype were used. (E) Representative H&E staining and follicle counting results (mean±s.e.m.) of ovaries from 6-month-old mice of each genotype. Scale bar: 500 µm. CL, corpus luteum. At least three mice of each genotype were used.

suggests that is has a possible role in meiotic progression events, such as spindle organization and chromosome segregation.

Generation of mutant mice with oocyte-specific deletion of *Ppp6c*

To explore the *in vivo* role of PP6c and its function in oocyte meiotic maturation, we decided to use the conditional knockout approach owing to the early lethality of PP6-deficient embryos. The Cre-LoxP site-specific recombination system was used to target *Ppp6c* for oocyte-specific deletion in mice. We first generated *Ppp6c*$^{F/F}$ mice in which exons II–IV of the *Ppp6c* gene were flanked with *Loxp* sites (Fig. S1). To generate the *Ppp6c*-targeting vector, a single *LoxP* site was introduced upstream of exon 2 of the *Ppp6c* gene, and an *Frt-Neomycin-Frt-LoxP* cassette was inserted into intron 4 (Fig. S1A). This targeting vector was electroporated into mouse embryonic stem cells (ESCs). The homologous recombinant ESC clones were analyzed by Southern blotting (Fig. S1B), and injected into blastocysts to generate chimeric mice. The chimeric mice exhibited germline transmission of the *LoxP-Neo Ppp6c* allele (*Ppp6c*$^{Fn/+}$). The *Ppp6c*$^{Fn/+}$ mouse was bred with the Flpe deleter mouse line (Farley et al., 2000) to excise the *Frt*-flanked neomycin cassette and generate the *Ppp6c* floxed heterozygous mouse (*Ppp6c*$^{F/+}$; Fig. S1C). After one round of self-crossing, *Ppp6c*$^{F/F}$ mice were obtained.

Then, we crossed *Ppp6c*$^{F/F}$ mice with transgenic mice expressing *Zp3* promoter-mediated Cre recombinase to generate oocyte-specific conditional PP6c-knockout mice (referred to as *Ppp6c*$^{F/F}$*; ZCre+* mice, Fig. S1A). In *Zp3-Cre* mice, Cre is expressed in oocytes of primary follicles from postnatal day 5 onwards and in later developmental stages (Hu et al., 2012). Immunofluorescence analysis of oocytes from *Ppp6c*$^{F/F}$*;ZCre+* females revealed loss of PP6c localization on chromosomes, indicating successful disruption of *Ppp6c* (Fig. 2A). Furthermore, by analyzing western blots, we confirmed that expression of the *Ppp6c* gene in germinal vesicle oocytes from *Ppp6c*$^{F/F}$*;ZCre+* females was absent (Fig. 2B).

PP6c is essential for female fertility

To investigate the effect of oocyte-specific knockout of PP6c on female fertility, a breeding assay was carried out by mating *Ppp6c*$^{F/F}$ or *Ppp6c*$^{F/F}$*;ZCre+* female mice with males of proven fertility for 6 months. As shown in Fig. 2C, female *Ppp6c*$^{F/F}$*;ZCre+* mice were

Journal of Cell Science (2015) 128, 3769-3780 doi:10.1242/jcs.173179

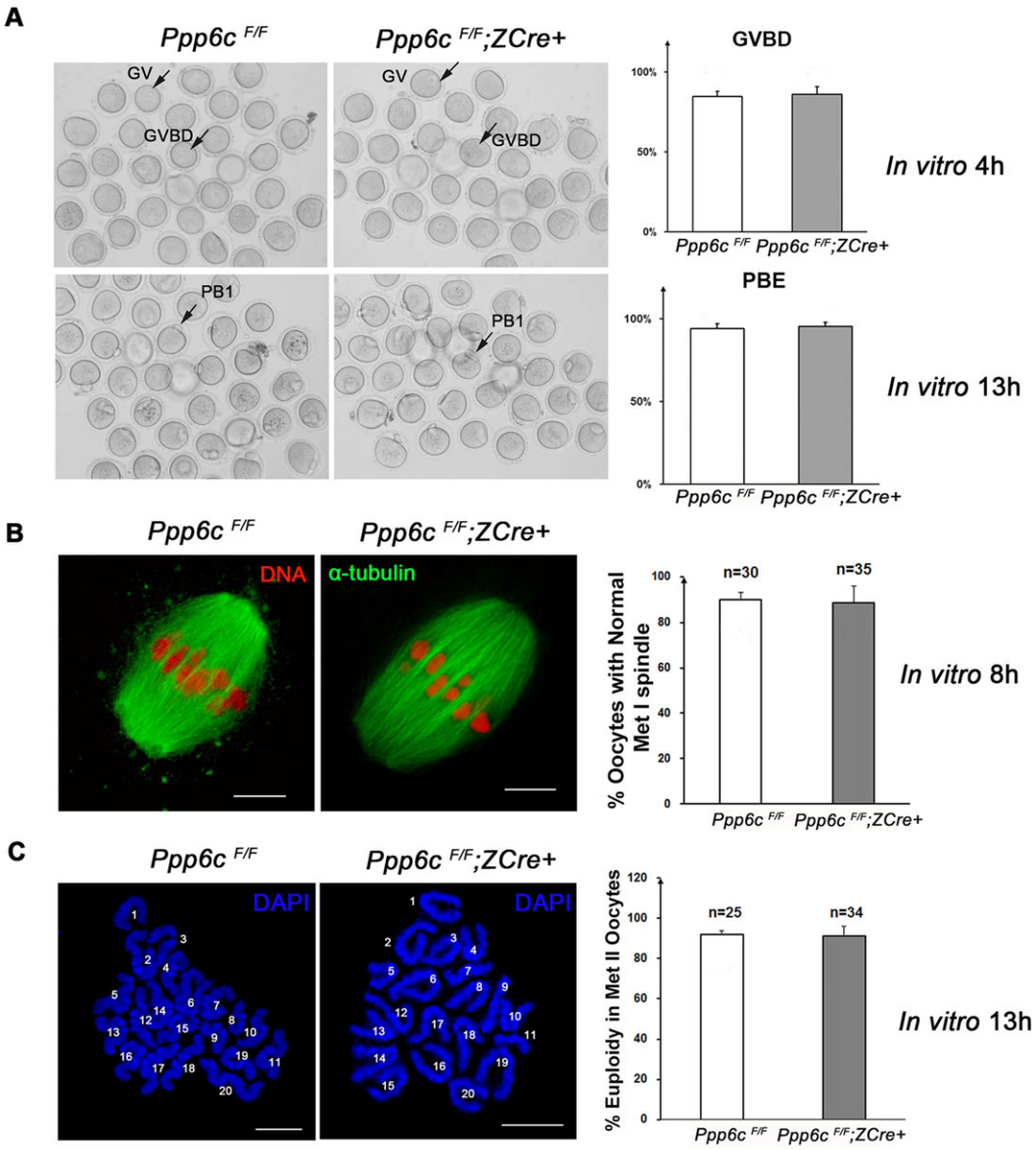

Fig. 3. PP6c depletion does not impair oocyte meiotic progression during the first meiosis. (A) Comparable GVBD rates and PBE rates of *Ppp6c*$^{F/F}$ oocytes and *Ppp6c*$^{F/F}$*;ZCre+* oocytes. Germinal vesicle (GV) oocytes were isolated and matured *in vitro*, oocytes that resumed meiosis I (GVBD) and extruded the first polar body (PBE) were counted at 4 h and 13 h, respectively. Representative DIC images are shown. Data are presented as mean±s.e.m. *In vitro* maturation (IVM) experiments were repeated at least three times; ≥150 oocytes of each genotype were analyzed for each time point. (B) Representative images of staining for DNA (red) and immunostaining for α-tubulin (green) showing normal spindle assembly in *Ppp6c*$^{F/F}$*; ZCre+* oocytes at the metaphase-I (Met I) stage. Scale bars: 10 µm. Germinal vesicle oocytes were isolated, cultured for 8 h to the metaphase-I stage and then fixed. The percentages of oocytes with a normal spindle at the MI stage of each genotype are presented as mean±s.e.m. The numbers of analyzed oocytes are indicated (*n*). (C) Chromosome spread of metaphase-II (Met II) oocytes from *Ppp6c*$^{F/F}$ and *Ppp6c*$^{F/F}$*; ZCre+* mice, showing chromosomes stained with DAPI (blue). Representative images are shown. Scale bars: 10 µm. Germinal vesicle oocytes were isolated and cultured for 13 h and metaphase-II oocytes with PB1 were fixed. The number of chromosomes from each oocyte was counted and the percentage showing euploidy (i.e. 20 pairs of chromatids) in metaphase-II oocytes of each genotype are presented as mean±s.e.m. The total numbers of analyzed oocytes are indicated (*n*).

severely subfertile and gave birth to about 66% fewer pups than *Ppp6c*$^{F/F}$ mice. The significant decrease of fertility in *Ppp6c*$^{F/F}$*;ZCre* + mice appeared not to be related to the ovulation rate since the mutant mice could ovulate approximately the same number of eggs (8.5±1.4) compared with control mice (8.7±0.8) in natural ovulation assays (mean±s.e.m.; Fig. 2D). Furthermore, we performed histological analysis and compared follicular development in *Ppp6c*$^{F/F}$*;ZCre+* mice to that in *Ppp6c*$^{F/F}$ mice. No apparent morphological difference was found in ovaries of both genotypes from 6-month-old mice, consistent with the follicle counting result (Fig. 2E). These data reveal that *Ppp6c* deletion from oocytes from the primary follicle stage does not affect follicular development, suggesting that the subfertility of *Ppp6c*$^{F/F}$*;ZCre+* mice is caused by defects in oocytes.

Depletion of PP6c does not affect oocyte meiotic maturation progress

To understand the defects of *Ppp6c*$^{F/F}$*;ZCre+* oocytes, we employed oocyte *in vitro* culture to observe the major events during the meiotic maturation process. The absence of PP6c seemed to have no influence on the oocyte meiotic maturation rate

Journal of Cell Science (2015) 128, 3769-3780 doi:10.1242/jcs.173179

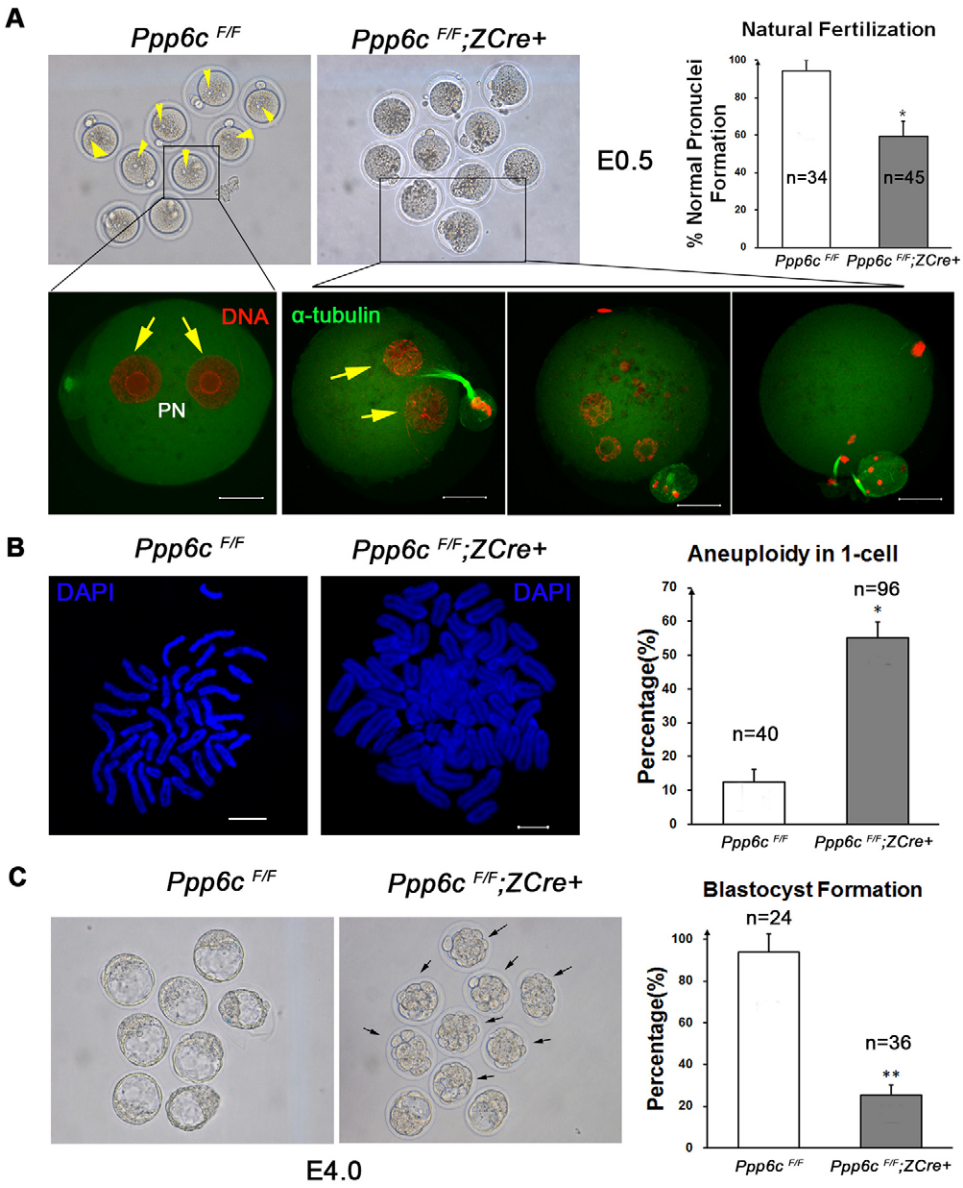

Fig. 4. Aneuploidy in zygotes leads to defective early embryonic development and subfertility in *Ppp6c*$^{F/F}$*;ZCre+* mice. (A) Representative images of zygotes at E0.5 from *Ppp6c*$^{F/F}$ and *Ppp6c*$^{F/F}$*;ZCre+* females. Yellow arrowheads show visible pronuclei. Representative images of immunostaining for DNA (red) and α-tubulin (green) showing pronuclei formation in zygotes from *Ppp6c*$^{F/F}$ and *Ppp6c*$^{F/F}$*;ZCre+* females are presented in the lower panel. Yellow arrows show normal pronuclei. PN, pronuclei. Scale bars: 20 µm. Percentages of zygotes with normal pronuclei formation at E0.5 in *Ppp6c*$^{F/F}$ and *Ppp6c*$^{F/F}$*;ZCre+* mice, presented as mean±s.e.m. At least five mice of each genotype were used and the total numbers of analyzed zygotes are indicated (*n*). **P*<0.05 (Student's *t*-test) (B) Chromosome spread of one-cell embryos blocked at metaphase with colchicine from *Ppp6c*$^{F/F}$ and *Ppp6c*$^{F/F}$*;ZCre+* female mice, showing chromosomes stained with DAPI (blue). Representative images are shown. Scale bars: 10 µm. The number of chromosomes of each embryo was counted and the percentage (mean±s.e.m.) of one-cell embryos with aneuploidy in the control group and mutant group is shown. The total numbers of analyzed embryos are indicated (*n*). **P*<0.05 (Student's *t*-test). (C) Representative images of embryos at E4.0 from *Ppp6c*$^{F/F}$ and *Ppp6c*$^{F/F}$*;ZCre+* females. Black arrows show apoptotic embryos. Percentages of blastocyst formation at E4.0 in *Ppp6c*$^{F/F}$ and *Ppp6c*$^{F/F}$*;ZCre+* mice, presented as mean±s.e.m. At least four mice of each genotype were used and the total numbers of analyzed embryos are indicated (*n*). ***P*<0.001 (Student's *t*-test).

because the *Ppp6c*$^{F/F}$*;ZCre+* oocytes exhibited normal GVBD rates (84.8±3.2%) and PBE rates (94.3±2.8%) compared with the *Ppp6c*$^{F/F}$ oocytes (86.1±4.8% and 95.5±2.5%) when cultured *in vitro* (mean± s.e.m.; Fig. 3A). Moreover, after 8 h of *in vitro* maturation, in *Ppp6c*$^{F/F}$*;ZCre+* oocytes spindles were well organized with chromosomes all aligned at the equatorial plate, showing no obvious difference compared to *Ppp6c*$^{F/F}$ oocytes, which was confirmed further by quantification (90.0±3.0% versus 88.6±7.1%) (Fig. 3B). To test whether chromosomes segregated correctly in the first meiosis after PP6c depletion, we employed chromosome spreading of metaphase-II oocytes after 13 h of *in vitro* culture and counted the number of chromosomes that showed no difference between the mutant group and the control group (92.0±1.8% versus 91.2±5.0%) (Fig. 3C). In addition, when we induced superovulation of the *Ppp6c*$^{F/F}$*;ZCre+* mice with pregnant mare serum gonadotropin (PMSG) and human chorionic gonadotropin (hCG) treatment, we could collect normal metaphase-II oocytes with visible first polar bodies, which suggests that the *Ppp6c*$^{F/F}$*;ZCre+* oocytes can undergo meiotic resumption and polar body emission *in vivo,* as well as *in vitro*. Therefore, PP6c might be dispensable for oocyte meiotic resumption and completion of the first meiosis.

Loss of PP6c leads to defective early embryonic development and subfertility

To find the causes for female subfertility in *Ppp6c*$^{F/F}$*;ZCre+* mice, we extended our observation of the *Ppp6c*$^{F/F}$*;ZCre+* oocytes after fertilization. *In vivo* zygotes from *Ppp6c*$^{F/F}$ and *Ppp6c*$^{F/F}$*;ZCre+* females were collected at embryonic day (E)0.5 and investigated. In contrast to fertilized *Ppp6c*$^{F/F}$ eggs, which had extruded the second polar bodies and showed two visible pronuclei (yellow arrowheads, Fig. 4A), a large proportion of zygotes from *Ppp6c*$^{F/F}$*;ZCre+* mice were abnormal with aberrant second polar body extrusion and no visible pronuclei (Fig. 4A). Further immunofluorescence analysis showed that only 59.4±8.2% (mean±s.e.m.) mutant zygotes displayed two pronuclei, significantly less than in the control group (94.4±5.6%), and the other 40.6% displayed various kinds of anomalies: some had more than two small pronuclei and some had accumulated chromatin without formation of pronuclei (Fig. 4A). The *Ppp6c*$^{F/F}$*;ZCre+* oocytes appeared to have defects in

Journal of Cell Science (2015) 128, 3769-3780 doi:10.1242/jcs.173179

completing MII. To confirm this observation, we performed chromosome spreading of 1-cell embryos that were arrested at metaphase by colchicine. As expected, up to 55.2±4.7% of mutant 1-cell embryos showed aneuploidy, significantly higher than that of control 1-cell embryos which displayed only 12.5±3.6% aneuploidy (Fig. 4B). Therefore, the chances of survival were quite small for the early embryos derived from *Ppp6c*$^{F/F}$*;ZCre+* females mated with WT males. As shown in Fig. 4C, at E4.0, almost all of the early embryos had reached the blastocyst stage with an obvious blastocoel in the control group (93.8±8.8%), but in the mutant group the embryos had barely reached the blastocyst stage (25.2±4.8%) and exhibited obvious malformation (black arrows). The above data indicated that defective early embryonic development derived from mutant zygotes with high aneuploidy rates may account for the main reasons for subfertility in *Ppp6c*$^{F/F}$*;ZCre+* mice. However, questions remained regarding specific defects in the *Ppp6c*$^{F/F}$*; ZCre+* oocytes that caused the aneuploidy concerning MII.

Depletion of PP6c impairs spindle shape in MII

To answer the question and unveil the role of PP6c in MII, we collected and observed superovulated metaphase-II oocytes using immunofluorescent analysis. As shown in Fig. 5A, *Ppp6c*$^{F/F}$ metaphase-II oocytes showed well-organized bipolar spindles with clearly detectable microtubule fibers and tightly aligned chromosomes at the metaphase plate; surprisingly, *Ppp6c*$^{F/F}$*; ZCre+* oocyte spindles displayed rather odd formations with several distinct arrays of bundled microtubules, though the chromosomes seemed to be aligned well. We suspected that the microtubules which formed the abnormal spindles in the *Ppp6c*$^{F/F}$*; ZCre+* oocytes might be excessively polymerized. So we cold-treated the metaphase-II oocytes from both groups at 4°C to depolymerize the cold-labile microtubules. When cold-treated for 15 min, no significant differences were found between *Ppp6c*$^{F/F}$ oocytes and *Ppp6c*$^{F/F}$*; ZCre+* oocytes; relatively cold-stable k-fibers still existed in both groups (white arrowheads, Fig. 5B). But after an extended cold treatment of 20 min, almost the entire spindle including k-fibers, which are normally resistant to cold over shorter periods, disappeared in the *Ppp6c*$^{F/F}$ oocytes; however, the spindles of *Ppp6c*$^{F/F}$*; ZCre+* oocytes still remained relatively intact (26.9±5.6% versus 76.6±6.1%; mean±s.e.m.), suggesting that these microtubule bundles were very stable, relatively resistant to cold and could not be depolymerized easily (Fig. 5B). Therefore, the experiments show that PP6c is required for maintaining a normal MII spindle organization.

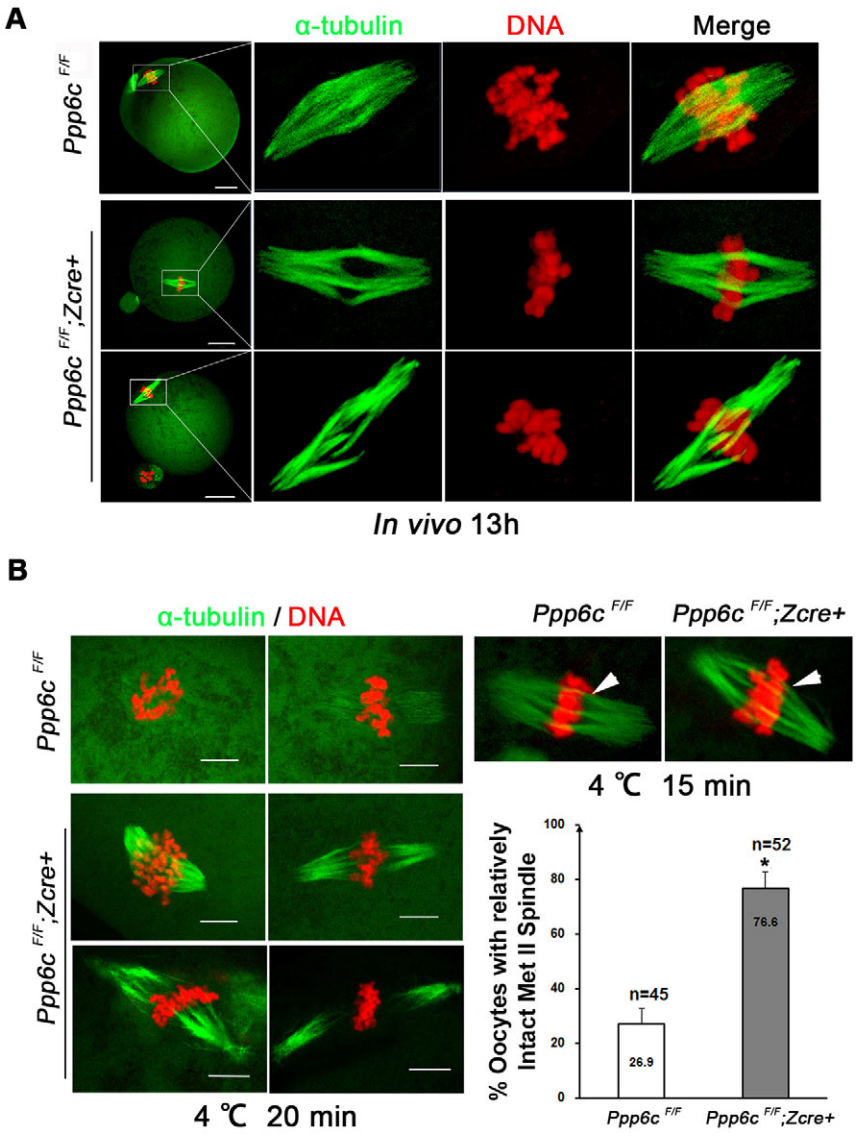

Fig. 5. Deficiency of PP6c resulted in abnormal spindle microtubules in MII. (A) Representative images of staining for DNA (red) and immunostaining for α-tubulin (green) showing spindle organization in super-ovulated metaphase-II (Met II) oocytes from *Ppp6c*$^{F/F}$ and *Ppp6c*$^{F/F}$*;ZCre+* mice after treatment with hCG. Scale bars: 20 µm. Magnifications of the boxed regions are shown. All of the experiments were repeated at least three times, and ≥50 oocytes of each genotype were analyzed. (B) Super-ovulated metaphase-II oocytes from *Ppp6c*$^{F/F}$ and *Ppp6c*$^{F/F}$*;ZCre+* mice were cold-treated at 4°C for 20 min and then fixed and double-stained for DNA (red) and α-tubulin (green) to show spindle microtubule depolymerization. All of the experiments were repeated at least three times, and representative results are shown. Scale bars: 10 µm. Representative images after cold treatment for 15 min are shown as a negative control to demonstrate that *Ppp6c*$^{F/F}$ oocytes do indeed have k-fibers. White arrowheads show k-fibers, which are relatively cold-stable microtubules associated with kinetochores. The percentages of oocytes with relatively intact spindles in the control group and mutant group after 20 min of cold treatment are presented as mean±s.e.m. The numbers of analyzed oocytes are indicated (*n*). **P*<0.05 (Student's *t*-test).

Journal of Cell Science (2015) 128, 3769-3780 doi:10.1242/jcs.173179

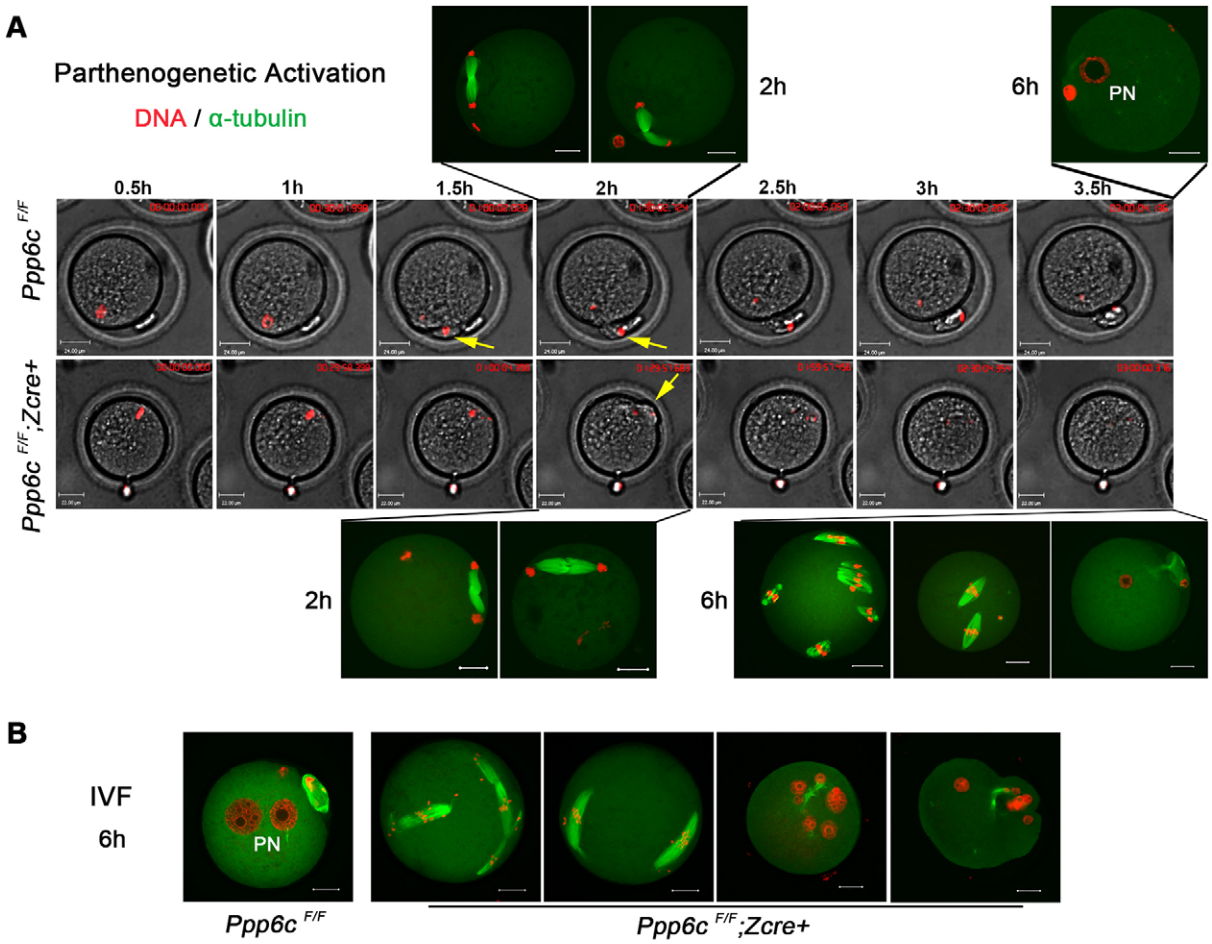

Fig. 6. *Ppp6c* deletion in oocytes causes failure of MII exit. (A) Dynamics of MII exit in *Ppp6c*$^{F/F}$ oocytes and *Ppp6c*$^{F/F}$*;ZCre+* oocytes. Super-ovulated metaphase-II oocytes were parthenogenetically activated and cultured in $SrCl_2$ activation medium supplemented with Hoechst 33342 (5 ng/ml) for 0.5 h and then were live imaged. Representative still images from Movies 1 and 2 are shown. Timestamps indicate hours after activation. Yellow arrows point at the second polar body extrusion. Red, DNA. Representative images of staining for DNA (red) and immunostaining for α-tubulin (green) showing spindle organization and chromatids separation at telophase II (2 h) and pronucleus formation (6 h) in activated oocytes of each genotype are also presented. All of the experiments were repeated at least three times, and ≥100 oocytes of each genotype were analyzed. PN, pronuclei. (B) Representative images of immunostaining for DNA (red) and α-tubulin (green) showing pronuclei formation in zygotes from *Ppp6c*$^{F/F}$ and *Ppp6c*$^{F/F}$*;ZCre+* mice. Super-ovulated metaphase-II oocytes of each genotype were collected and fertilized *in vitro* with active spermatozoa. Zygotes were cultured for 6 h after IVF and then fixed. All of the experiments were repeated at least three times, and ≥110 oocytes of each genotype were analyzed. PN, pronuclei. Scale bars: 20 µm.

Oocyte-specific deletion of *Ppp6c* causes failure of MII exit

Considering such abnormalities of *Ppp6c*$^{F/F}$*;ZCre+* oocytes, we asked if they could succeed in MII exit. So we treated oocytes with $SrCl_2$ activation solution to activate the metaphase-II-arrested oocytes and started to observe the completion process of meiosis II by live-cell imaging after 30 min of activation. As shown in Fig. 6A, the control metaphase-II oocytes were activated and entered anaphase II around 1.5 h, and completed cytokinesis around 2 h (Movie 1). In comparison, *Ppp6c*$^{F/F}$*;ZCre+* oocytes were able to enter anaphase II and had a tendency to extrude the second polar body, but then the extruding polar body retracted and cytokinesis failed eventually with the chromatids still left in the oocytes (Movie 2). In the meantime, the oocytes in both groups were also fixed and stained with α-tubulin and propidium iodide at 2 h or 6 h of parthenogenetic activation to observe the separation of sister chromatids or pronuclei formation, respectively. Indeed, the immunofluorescence analysis results confirmed the live-cell imaging observations in greater detail. At 2 h, in both groups sister chromatids had segregated and moved to the spindle poles indicating that anaphase or telophase II had been reached, but spindles in the mutant group appeared twisted or loosened without displaying a visible tight contractile ring. At 6 h, unlike control eggs in which large pronuclei had formed with a low abnormality rate (14.8±4.7%; mean±s.e.m.), up to 65.7±5.6% mutant eggs displayed two or more spindles in the vicinity of every chromatid accumulation, or much smaller pronuclei were displayed. In addition, we performed *in vitro* fertilization (IVF) experiments to confirm the above observation and obtained consistent results. At 6 h after IVF, the abnormal mutant zygotes contained either two or more spindles, or several small pronuclei (Fig. 6B). Taken together, these data demonstrate that PP6c is indispensable for MII exit.

Aurora A activity is upregulated in PP6c-deficient oocytes

Based on the above results, the main cause for the PP6c depletion phenotype appears to be defects in the MII spindle. As a crucial regulator of spindle organization, Aurora A is activated by the spindle assembly factor TPX2 and they form a complex together (Bayliss et al., 2003). PP6 has been reported to be a T-loop phosphatase for the Aurora-A–TPX2 complex at T288 of Aurora A during mitosis (Zeng et al., 2010), and the effects of PP6

Journal of Cell Science (2015) 128, 3769-3780 doi:10.1242/jcs.173179

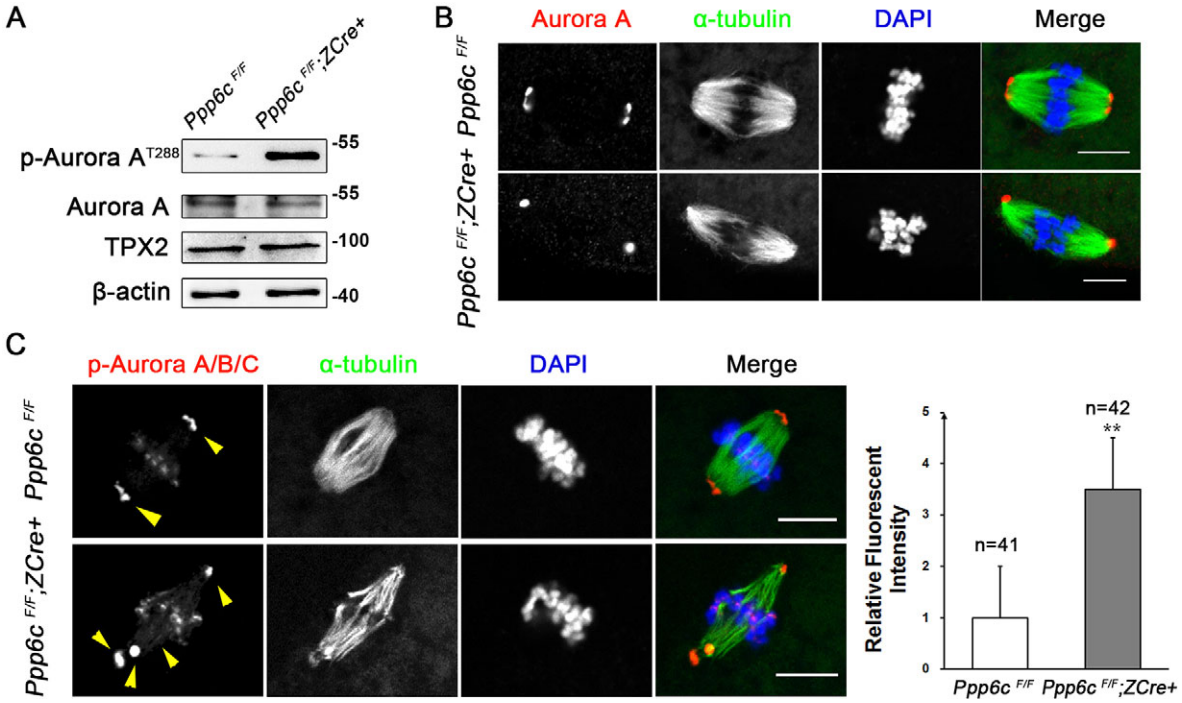

Fig. 7. Amplified Aurora A activity in PP6c-deficient metaphase-II oocytes. (A) Western blots showing upregulated p-Aurora A T288 in *Ppp6c*$^{F/F}$*;ZCre+* oocytes. Each sample (200 metaphase-II oocytes) was collected after being cultured for 13 h *in vitro*, and immunoblotted for p-Aurora A^{T288}, Aurora A, TPX2 and β-actin. The level of β-actin was used as internal control. Molecular mass is given in kDa. (B) Representative images of immunostaining for Aurora A (red), α-tubulin (green) and staining of DNA (blue) showing comparable signals of total Aurora A in metaphase-II oocytes from *Ppp6c*$^{F/F}$ and *Ppp6c*$^{F/F}$*;ZCre+* mice. Scale bars: 10 µm. Experiments were repeated at least three times and ≥30 oocytes of each genotype were analyzed. (C) Representative immunofluorescence staining showing the amplified p-Aurora A^{T288} signal at spindle poles in PP6c-depleted metaphase-II oocytes. Red, phosphorylated Aurora A, B and C; green: α-tubulin; blue, DNA. Yellow arrowheads show specific p-Aurora A^{T288}signals. Scale bars: 10 µm. Quantification of the p-Aurora A T288 signal at spindle poles were presented as the mean±s.e.m. Experiments were repeated at least three times and the numbers of analyzed oocytes are indicated (*n*). ***P*<0.001 (Student's *t*-test).

inactivation on the Aurora-A–TPX2 complex were therefore investigated. Western blot analysis using an antibody for Aurora A phosphorylated at T288 (p-Aurora A^{T288}) demonstrated that Aurora A activity was significantly amplified in *Ppp6c*$^{F/F}$*;ZCre+* metaphase-II oocytes, although the expression of Aurora A and TPX2 seemed unchanged (Fig. 7A). We also performed immunofluorescence experiments to test the effect of PP6c deficiency on Aurora A localization and activity. In *Ppp6c*$^{F/F}$ metaphase-II oocytes, the staining of Aurora A was spread at the spindle poles, whereas in *Ppp6c*$^{F/F}$*;ZCre+* oocytes the staining was concentrated into a big dot at each pole, but this staining was not stronger than that in control oocytes (Fig. 7B). As for staining of p-Aurora A^{T288} at the spindle poles, it was clearly elevated and had spread to the spindle microtubules in PP6c-deficient oocytes in contrast to the control oocytes (Fig. 7C, yellow arrowheads). Results from both methods confirm that Aurora A activity is upregulated in metaphase-II oocytes when PP6 function is abolished.

Aurora A inhibition rescues the PP6c depletion phenotype

MLN8237 has been proven to be a highly specific small-molecule inhibitor of Aurora A (Manfredi et al., 2011), and we used this drug in a rescue strategy for the PP6c depletion phenotype. A low dose of MLN8237 (20 nM) was added to M2 culture medium and the oocytes were matured *in vitro* and collected for western blot and immunofluorescence experiments. Addition of 20 nM MLN8237 reversed the increase of p-Aurora A^{T288} in metaphase-II oocytes after PP6c depletion (Fig. 8A). Importantly, this partial Aurora A inhibition also rescued the impaired spindle shape in *Ppp6c*$^{F/F}$*;ZCre+* metaphase-II oocytes, which now showed normal barrel-shaped spindles with normal levels of p-Aurora A^{T288} staining just like the *Ppp6c*$^{F/F}$ oocytes (Fig. 8B). To further test the rescue effect of Aurora A inhibition, we carried out IVF experiments with super-ovulated metaphase-II oocytes after a short treatment with 20 nM MLN8237 for 15 min. As seen in Fig. 8C, after MLN8237 treatment, many more zygotes from mutant groups had formed normal pronuclei (white arrows) compared to those without treatment. Statistically, the Aurora A inhibition treatment significantly improved the normal pronuclei formation rate from 42.7% to 72.3%. The reversal of the PP6c depletion phenotype upon reduction of Aurora A activity using MLN8237 indicates that Aurora A is a major substrate of PP6 during MII in mouse oocytes.

Collectively, these findings are in support of PP6 acting as a crucial regulator for MII spindle organization by limiting the activity of Aurora A, and show that PP6 is essential for efficient MII exit and correct embryo euploidy, providing an evident explanation for female subfertility in the absence of functional PP6c.

DISCUSSION

In female reproduction, production of quality eggs requires both successful ovulation and precise oocyte meiotic completion. By crossing *Ppp6c*$^{F/F}$ mice with *Zp3-Cre* mice to generate mutant mice with specific deletion of *Ppp6c* in oocytes, we were able to investigate the roles of PP6c in both ovulation and meiosis. We found that mutant mice with *Ppp6c* deletion in oocytes from primary follicle stages could ovulate normally, but still suffered severe female subfertility. A step-by-step investigation of the meiosis process in *Ppp6c*$^{F/F}$*;ZCre+* oocytes showed that a disorganized MII spindle, failed MII exit and high-frequency

Journal of Cell Science (2015) 128, 3769-3780 doi:10.1242/jcs.173179

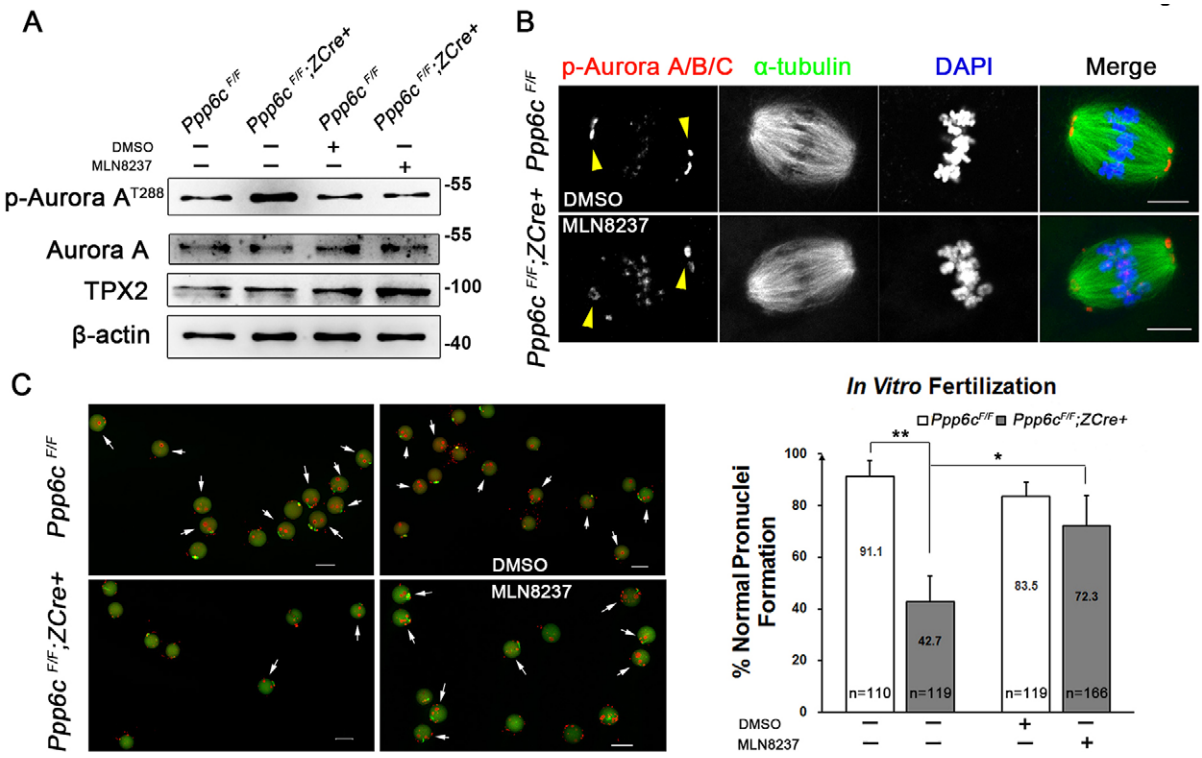

Fig. 8. Aurora A inhibition by MLN8237 rescues the PP6c depletion phenotype. (A) Western blots showing that enhanced Aurora A activity in *Ppp6c*$^{F/F}$*;ZCre+* oocytes was downregulated to the normal level after MLN8237 treatment. Each sample (200 metaphase-II oocytes) was collected after being cultured for 13 h with or without treatment (20 nM DMSO for *Ppp6c*$^{F/F}$ oocytes and 20 nM MLN8237 for *Ppp6c*$^{F/F}$*;ZCre+* oocytes), and immunoblotted for p-Aurora A^{T288}, Aurora A, TPX2 and β-actin. The level of β-actin was used as internal control. Molecular mass is given in kDa. (B) Representative immunofluorescence staining showing rescued spindle shape and a reduced p-Aurora A^{T288} signal at spindle poles in PP6c-depleted metaphase-II oocytes after MLN8237 treatment. Red, phosphorylated Aurora A, B and C; green: α-tubulin; blue, DNA. Yellow arrowheads point at p-Aurora A^{T288} signals. Experiments were repeated at least three times and ≥30 oocytes of each genotype were analyzed. Scale bars: 10 µm. (C) Representative immunofluorescence staining images showing improved pronuclei formation in mutant zygotes at IVF 6 h after MLN8237 treatment. Super-ovulated metaphase-II oocytes of each genotype were collected and cultured in M2 medium with or without treatment for 15 min (20 nM DMSO for *Ppp6c*$^{F/F}$ oocytes and 20 nM MLN8237 for *Ppp6c*$^{F/F}$*;ZCre+* oocytes). Then the oocytes were washed and fertilized *in vitro* with active spermatozoa. Zygotes were cultured for 6 h before fixation. Green, α-tubulin; Red, DNA. White arrows show zygotes with normal pronuclei formation. Scale bars: 100 µm. Percentages of zygotes with normal pronuclei formation in each group are presented as mean±s.e.m. All of the experiments were repeated at least three times and the total numbers of analyzed zygotes are indicated (*n*). **P*<0.05; ***P*<0.001 (Student's *t*-test).

aneuploidy in zygotes were underlying causes for this subfertility.

Meiosis is the cellular process by which haploid gametes are generated from diploid cells. Strikingly, female germ cell meiosis is characterized by two rounds of cell cycle arrests and asymmetric cell divisions in both meioses. The first meiotic division, with the separation of homologous chromosomes is termed reductional division. The second division, which takes place immediately after MI without an intervening S-phase, is equational, with the separation of sister chromatids, similar to mitosis (Schindler, 2011; Wassmann, 2013). Although unique, oocyte meiosis, and especially MII, still appears to adopt many of the same proteins and mechanisms as described for mitosis, with necessary modifications to accommodate their special needs (Liu, 2012). Among numerous kinases in somatic cells, Aurora kinases are a family of serine/threonine protein kinases required for successful execution of cell division by ensuring the formation of a bipolar mitotic spindle, accurate segregation of chromosomes and the completion of cytokinesis (Crane et al., 2004). Aurora A is the most abundantly expressed Aurora kinase in mouse oocytes (Swain et al., 2008). As an important regulator involved in the G2/M transition, centrosome maturation and separation, and spindle formation in somatic cells, not surprisingly, Aurora A also functions in meiosis. Similar to mitotic cells, Aurora A localizes to microtubule-organizing centers (MTOCs) and spindle poles during MI and MII and its activated form (phosphorylated on T288) associates with poles prior to and after GVBD (Saskova et al., 2008). Overexpression of Aurora A leads to increased numbers of MTOCs, formation of an abnormal MI spindle and failed metaphase-I–metaphase-II transition (Saskova et al., 2008; Yao et al., 2004). Importantly, we showed that PP6 appears to act as an Aurora A suppressor and PP6 dysfunction would upregulate Aurora A activity and damage spindle formation during MII, similar to effects of Aurora A overexpression. Hence, the question arises as to why only MII, and not MI, was affected in PP6c-depleted oocytes? Now we have to consider TPX2, a known activator of Aurora A in mitotic cells. PP6 specifically recognizes and acts upon the Aurora-A–TPX2 complex as the T-loop phosphatase regulating Aurora A activity (Zeng et al., 2010). Along with the specific expression pattern of TPX2, which accumulates from MI and is most expressed at MII (Brunet et al., 2008), we can assume that the Aurora-A–TPX2 complex forms and functions mainly in MII, which would make the spindle formation in MII more sensitive to the absence of PP6 than in MI. Another possibility is that Aurora A activity could be regulated by PP1 or PP2A in MI and mainly by PP6 in MII given that PP1 and PP2A can act as free Aurora A phosphatases (Bayliss et al., 2003; Eyers et al., 2003; Tsai et al., 2003). This could explain why the PP6c-deficient phenotype is only exhibited during MII and thereafter. Furthermore,

Journal of Cell Science (2015) 128, 3769-3780 doi:10.1242/jcs.173179

our evidence also confirms that the mechanisms for spindle formation in MI and MII might be different, which demonstrates the complexity and unique charm of meiosis in oocytes.

Recently the role of PP6 in mitosis has been studied in great detail (Hammond et al., 2013; Zeng et al., 2010), and the T-loop of Aurora A has been identified as the key target of PP6 in mitosis. The knowledge gained from these studies has benefited our analysis of Aurora A as a potential substrate in our study, and in fact our study also confirmed that Aurora A is a crucial target for PP6, not only in mitosis but also in meiosis, which is a very interesting and remarkable finding. Aside from sharing the same target, PP6 also has similar behaviors in mitosis and meiosis; for example, PP6 regulates spindle formation in both kinds of cell division, because efficient PP6c depletion causes spindle formation and chromosome segregation defects and results in a high risk of micronucleation or binucleation in mitosis or egg aneuploidy in meiosis. However, there are also several differences of PP6 behavior in mitosis and meiosis. First, the subcellular localization of PP6 is not the same. In mitotic cells, PP6 is localized to the cytoplasm; however, it has a specific chromatin localization in oocytes. In our study, the loss of the chromatin localization in the mitotic one-cell embryos (Fig. 1B) also confirmed that PP6 has a unique location in meiosis. Second, the PP6c depletion phenotypes are not quite the same. PP6C-depleted somatic cells show delayed spindle formation and defective spindle integrity with highly fragmented and disordered spindle poles and fail to efficiently align chromosomes at the metaphase plate. However, these defects were not found in PP6c-depleted oocytes. In fact, in oocytes without PP6c, the MI spindles were totally normal and MII spindles, though abnormal, still remained intact with a bipolar organization and well-aligned chromosomes. Moreover, hyperstable spindles with excessively polymerized microtubules in PP6c-deficient oocytes have not been discovered in mitotic cells. The above different spindle defects might be due to functional variation of Aurora A in mitosis and meiosis II. Taken together, our study unveils a role of PP6 in meiosis that was hitherto unknown and provides a substantial advance in our knowledge on PP6 function.

As members of PP2A-like subfamily, PP6 does share common features with PP2A and PP4. They not only have a similar structure and similar sensitivities to small-molecule inhibitors, such as okadaic acid, but they also have similar functions. Like PP2A, these similarities might be the reason for unexplained PP6 functions for many years. Our study, by using genetically modified mouse models, provides convincing evidence showing important roles for PP6 in oocyte meiosis. From previous reports and our two conditional knockout studies of PP2A and PP6 in oocytes, we have demonstrated that PP6 is not merely 'PP2A-like'. In oocyte meiosis, PP2A mainly functions in meiosis I as a GVBD inhibitor and centromeric cohesion protector, and also plays a role in metaphase-II arrest and egg activation (Chang et al., 2011); however, PP6 appears to mainly function in MII as an Aurora A kinase inhibitor that ensures proper spindle formation.

Female meiosis is error-prone in humans. It is estimated that 20% of human oocytes are aneuploid, and mistakes in meiotic chromosome segregation account for one third of all pregnancy losses (Hassold and Hunt, 2001; Qiao et al., 2014; Wang et al., 2011). Both MI and MII exits are key events in maintaining the euploidy of oocytes. Interestingly, all PP2A-like protein phosphatases have essential roles in preventing oocyte aneuploidy. Our previous study has reported that oocyte-specific deletion of *ppp2r1a* results in precocious separation of sister chromatids and oocyte aneuploidy, which provided direct *in vivo* evidence that PP2A ensures accurate chromosome segregation and euploidy during the MI exit (Hu et al., 2014). PP4 has been reported to be involved in the establishment or maintenance of chiasmata during meiotic prophase I and in regulating embryo microtubule severing in *C. elegans* (Han et al., 2009; Sumiyoshi et al., 2002). Here, we have shown that PP6c depletion in oocytes leads to defective MII spindle function and unfaithful chromatid segregation in MII, which proves that PP6 also acts as an important antagonist to oocyte aneuploidy during the MII exit. Our study contributes to elucidating the underlying mechanisms for proper spindle formation and accurate chromosome segregation.

In conclusion, for the first time, our study provides strong *in vivo* evidence from the whole animal level to the molecular level that PP6 in oocytes plays a unique role as an Aurora A suppressor in MII and is crucial for MII exit, euploid egg production and female fertility.

MATERIALS AND METHODS

Mice

Mice lacking *Ppp6c* in oocytes (referred to as *Ppp6c*$^{F/F}$*;ZCre*+) were generated by crossing *Ppp6c*$^{F/F}$ mice with *Zp3-Cre* mice. Generation of *Ppp6c* floxed heterozygous mouse was performed as follows. A 12-kb genomic fragment, comprising a 2.2-kb 5′ homologous arm, an 8-kb core region containing exons 2–4, and a 2-kb 3′ homologous arm, was cloned into a Pfrt1 vector containing an *Frt*-floxed neomycin resistance cassette and a TK cassette. The neomycin cassette was inserted downstream of exon 4, and the other LoxP element was inserted upstream of exon 2. A NotI-linearized targeting vector was electroporated into mouse ESCs. Correct targeting of ESCs was confirmed by a Southern blot analysis. The chimeric mice were generated by microinjection of targeted ESCs into C57BL/6J blastocysts. The mice were housed under controlled environmental conditions with free access to water and food. Light was provided between 08:00 and 20:00. Animal care and handling were conducted according to the guidelines of the Animal Research Committee of the Institute of Zoology, Chinese Academy of Sciences.

Reagents and antibodies

Commercial antibodies were used to detect α-tubulin (mouse, DM1A; Sigma-Aldrich), PPP6C (rabbit, A300-844A; Bethyl Laboratories, Inc.), Aurora A (rabbit, BS1840; Bioworld Technology, Inc.), phosphorylated Aurora-A, Aurora-B and Aurora-C (at T288, T232 and T198, respectively) (rabbit, 2914; Cell Signaling Technology), TPX2 (rabbit, 11741-1-AP; Proteintech Group, Inc.) and β-actin (mouse, sc-47778, Santa Cruz Biotechnology). Secondary antibodies were purchased from ZhongShan Golden Bridge Biotechnology Co. (Beijing, China). Aurora A kinase inhibitor was obtained from Selleck Chemicals (MLN8237) and was used at a working concentration of 20 nM (from a 500,000× stock).

Natural ovulation and superovulation

For the natural ovulation assay, 2- to 4-month-old female mice were mated with fertile males overnight. Successful mating was confirmed by the presence of vaginal plugs. Fertilized eggs were harvested from oviducts, and counted and analyzed after treatment of the cumulus mass with 1 mg/ml hyaluronidase (Sigma-Aldrich) in M2 medium (Sigma-Aldrich). Blastocysts were harvested from the uterus at E3.5 and counted.

To induce ovulation and collect metaphase-II oocytes, each female mouse was injected with 10 IU of PMSG followed by 10 IU of hCG 48 h to promote ovulation. Mice were killed at 12–14 h of hCG treatment and cumulus–oocyte complexes (COCs) were recovered from each oviduct. After a 5-min treatment with hyaluronidase (1 mg/ml) in M2 medium, oocytes were collected.

Histological analysis and quantification of ovarian follicles

Ovaries used for histological analysis were collected from adult female mice. Then, they were fixed in 4% paraformaldehyde (pH 7.5) overnight at 4°C, dehydrated and embedded in paraffin. Paraffin-embedded ovaries were

sectioned at a thickness of 8 µm for hematoxylin and eosin (H&E) staining. One or both ovaries from more than three mice of each genotype were used for the analysis. Quantification of ovarian follicles was performed as previously described (Hu et al., 2014).

Parthenogenetic activation and IVF

For Sr^{2+} activation, super-ovulated metaphase-II oocytes were first washed twice in M2 medium and once in activation medium and then cultured in activation medium (Ca^{2+}-free CZB medium supplemented with 10 mM $SrCl_2$) for 6 h.

In vitro fertilization (IVF) was performed by recovering fresh sperm from C57BL6 male mice from the epididymis into HTF medium for at least 0.5 h. Then the dispersed sperm cells were added into the HTF drops containing the mature COCs. After co-incubation for 2 h, presumptive zygotes were washed three times to remove cumulus cells and excess sperm, and placed into 20-µl drops of HTF medium under mineral oil. Embryos were cultured at 37°C in a humidified atmosphere of 5% O_2 and 6% CO_2 in air for another 4 h and collected for assessment.

Live imaging of oocyte activation

For live-cell imaging, super-ovulated metaphase-II oocytes were activated and cultured in activation medium supplemented with Hoechst 33342 (5 ng/ml) for 0.5 h and then transferred to the PerkinElmer precisely Ultra VIEW VOX Confocal Imaging System (PerkinElmer) equipped with 37°C incubator and 5% CO_2 supply (Jiang et al., 2014). The observation lasted for at least 7 h. The DNA in oocytes was labeled in blue using Hoechst 33342, and changed into red in the figures and movies.

Oocyte collection and culture

Germinal vesicle stage oocytes were isolated from ovaries of 6- to 9-week-old female mice and cultured in M2 medium under paraffin oil at 37°C, 5% CO_2 in air. For Aurora A inhibition, 20 nM MLN8237 or control DMSO was added to M2 medium for oocyte culture. Oocytes were collected at different times of culture for immunofluorescence staining, western blotting and chromosome spreads.

Immunofluorescence analysis and chromosome spread

Oocytes for immunofluorescence staining were fixed in 4% paraformaldehyde in PBS for 30 min at room temperature. Then the fixed oocytes were transferred to membrane permeabilization solution (0.5% Triton X-100) for 20 min and blocking buffer (1% BSA-supplemented PBS) for 1 h. Finally, oocytes were incubated overnight at 4°C with the antibodies described above at appropriate dilutions. Then the oocytes were mounted on glass slides and examined with a laser scanning confocal microscope (Zeiss LSM 780 META, Germany).

For chromosome spreads, the oocytes were first freed of the zona pellucida by acid Tyrode's solution (Sigma-Aldrich). After a brief recovery in M2 medium, the oocytes were transferred onto glass slides and fixed in a solution of 1% paraformaldehyde in distilled H_2O (pH 9.2) containing 0.15% Triton X-100 and 3 mM dithiothreitol. DNA on the slides was stained with DAPI and slides were mounted for observation by immunofluorescence microscopy.

Western blot analysis

A total of 200 mouse oocytes or zygotes per sample were mixed with 2× SDS sample buffer and boiled for 5 min at 100°C for SDS-PAGE. Western blotting was performed as described previously (Qi et al., 2013), using the antibodies against PPP6c, Aurora A and TPX2 at 1:500, antibody against phosphorylated Aurora A, B and C at 1:1000, and antibody against β-actin at 1:2000.

Statistical analysis

All experiments were repeated at least three times. Statistical analysis was performed using SPSS. Data are expressed as mean±s.e.m. and $P<0.05$ was considered statistically significant.

Acknowledgements

We thank Prof. Shao-Rong Gao for *Zp3-Cre* mice and Shi-Wen Li, Li-Juan Wang and Yi Hou for their technical assistance.

Competing interests

The authors declare no competing or financial interests.

Author contributions

Conception and design was undertaken by M.-W.H., Z.-B.W., X.X., X.Y. and Q.-Y.S. Execution was undertaken by M.-W.H., Y.T., Z.-Z.J., X.-S.M., N.H. and X.C. Interpretation of the data was undertaken by M.-W.H. Preparing the article was undertaken by M.-W.H., Z.-B.W., H.S., X.Y. and Q.-Y.S. All authors read and approved the manuscript for publication.

Funding

This work was supported by the National Basic Research Program of China [grant number 2012CB944404] and the National Natural Science Foundation of China [grant number 31530049, 31371451].

Supplementary information

Supplementary information available online at
http://jcs.biologists.org/lookup/suppl/doi:10.1242/jcs.173179/-/DC1

References

Bayliss, R., Sardon, T., Vernos, I. and Conti, E. (2003). Structural basis of Aurora-A activation by TPX2 at the mitotic spindle. *Mol. Cell* **12**, 851-862.

Brunet, S., Dumont, J., Lee, K. W., Kinoshita, K., Hikal, P., Gruss, O. J., Maro, B. and Verlhac, M.-H. (2008). Meiotic regulation of TPX2 protein levels governs cell cycle progression in mouse oocytes. *PLoS ONE* **3**, e3338.

Caenepeel, S., Charydczak, G., Sudarsanam, S., Hunter, T. and Manning, G. (2004). The mouse kinome: discovery and comparative genomics of all mouse protein kinases. *Proc. Natl. Acad. Sci. USA* **101**, 11707-11712.

Chang, H.-Y., Jennings, P. C., Stewart, J., Verrills, N. M. and Jones, K. T. (2011). Essential role of protein phosphatase 2A in metaphase II arrest and activation of mouse eggs shown by okadaic acid, dominant negative protein phosphatase 2A, and FTY720. *J. Biol. Chem.* **286**, 14705-14712.

Crane, R., Gadea, B., Littlepage, L., Wu, H. and Ruderman, J. V. (2004). Aurora A, meiosis and mitosis. *Biol. Cell* **96**, 215-229.

Douglas, P., Zhong, J., Ye, R., Moorhead, G. B. G., Xu, X. and Lees-Miller, S. P. (2010). Protein phosphatase 6 interacts with the DNA-dependent protein kinase catalytic subunit and dephosphorylates gamma-H2AX. *Mol. Cell. Biol.* **30**, 1368-1381.

Douglas, P., Ye, R., Trinkle-Mulcahy, L., Neal, J. A., De Wever, V., Morrice, N. A., Meek, K. and Lees-Miller, S. P. (2014). Polo-like kinase 1 (PLK1) and protein phosphatase 6 (PP6) regulate DNA-dependent protein kinase catalytic subunit (DNA-PKcs) phosphorylation in mitosis. *Biosci. Rep.* **34**, 257-271.

Eyers, P. A., Erikson, E., Chen, L. G. and Maller, J. L. (2003). A novel mechanism for activation of the protein kinase Aurora A. *Curr. Biol.* **13**, 691-697.

Farley, F. W., Soriano, P., Steffen, L. S. and Dymecki, S. M. (2000). Widespread recombinase expression using FLPeR (flipper) mice. *Genesis* **28**, 106-110.

Hammond, D., Zeng, K., Espert, A., Bastos, R. N., Baron, R. D., Gruneberg, U. and Barr, F. A. (2013). Melanoma-associated mutations in protein phosphatase 6 cause chromosome instability and DNA damage owing to dysregulated Aurora-A. *J. Cell Sci.* **126**, 3429-3440.

Han, X., Gomes, J.-E., Birmingham, C. L., Pintard, L., Sugimoto, A. and Mains, P. E. (2009). The role of protein phosphatase 4 in regulating microtubule severing in the Caenorhabditis elegans embryo. *Genetics* **181**, 933-943.

Hassold, T. and Hunt, P. (2001). To err (meiotically) is human: the genesis of human aneuploidy. *Nat. Rev. Genet.* **2**, 280-291.

Hirshfield, A. N. (1991). Development of follicles in the mammalian ovary. *Int. Rev. Cytol.* **124**, 43-101.

Hodis, E., Watson, I. R., Kryukov, G. V., Arold, S. T., Imielinski, M., Theurillat, J.-P., Nickerson, E., Auclair, D., Li, L., Place, C. et al. (2012). A landscape of driver mutations in melanoma. *Cell* **150**, 251-263.

Hosing, A. S., Valerie, N. C., Dziegielewski, J., Brautigan, D. L. and Larner, J. M. (2012). PP6 regulatory subunit R1 is bidentate anchor for targeting protein phosphatase-6 to DNA-dependent protein kinase. *J. Biol. Chem.* **287**, 9230-9239.

Hu, M.-W., Wang, Z.-B., Schatten, H. and Sun, Q.-Y. (2012). New understandings on folliculogenesis/oogenesis regulation in mouse as revealed by conditional knockout. *J. Genet. Genomics* **39**, 61-68.

Hu, M.-W., Wang, Z.-B., Jiang, Z.-Z., Qi, S.-T., Huang, L., Liang, Q.-X., Schatten, H. and Sun, Q.-Y. (2014). Scaffold subunit Aalpha of PP2A is essential for female meiosis and fertility in mice. *Biol. Reprod.* **91**, 19.

Janssens, V. and Goris, J. (2001). Protein phosphatase 2A: a highly regulated family of serine/threonine phosphatases implicated in cell growth and signalling. *Biochem. J.* **353**, 417-439.

Jiang, Z.-Z., Hu, M.-W., Wang, Z.-B., Huang, L., Lin, F., Qi, S.-T., Ouyang, Y.-C., Fan, H.-Y., Schatten, H., Mak, T.-W. et al. (2014). Survivin is essential for fertile egg production and female fertility in mice. *Cell Death Dis.* **5**, e1154.

Jones, K. T. (2005). Mammalian egg activation: from Ca2+ spiking to cell cycle progression. *Reproduction* **130**, 813-823.

Kajihara, R., Sakamoto, H., Tanabe, K., Takemoto, K., Tasaki, M., Ando, Y. and Inui, S. (2014). Protein phosphatase 6 controls BCR-induced apoptosis of WEHI-231 cells by regulating ubiquitination of Bcl-xL. *J. Immunol.* **192**, 5720-5729.
Kamoun, M., Filali, M., Murray, M. V., Awasthi, S. and Wadzinski, B. E. (2013). Protein phosphatase 2A family members (PP2A and PP6) associate with U1 snRNP and the spliceosome during pre-mRNA splicing. *Biochem. Biophys. Res. Commun.* **440**, 306-311.
Krauthammer, M., Kong, Y., Ha, B. H., Evans, P., Bacchiocchi, A., McCusker, J. P., Cheng, E., Davis, M. J., Goh, G., Choi, M. et al. (2012). Exome sequencing identifies recurrent somatic RAC1 mutations in melanoma. *Nat. Genet.* **44**, 1006-1014.
Liu, X. J. (2012). Polar body emission. *Cytoskeleton* **69**, 670-685.
Manfredi, M. G., Ecsedy, J. A., Chakravarty, A., Silverman, L., Zhang, M., Hoar, K. M., Stroud, S. G., Chen, W., Shinde, V., Huck, J. J. et al. (2011). Characterization of Alisertib (MLN8237), an investigational small-molecule inhibitor of aurora A kinase using novel in vivo pharmacodynamic assays. *Clin. Cancer Res.* **17**, 7614-7624.
Mehlmann, L. M. (2005). Stops and starts in mammalian oocytes: recent advances in understanding the regulation of meiotic arrest and oocyte maturation. *Reproduction* **130**, 791-799.
Moorhead, G. B. G., Trinkle-Mulcahy, L. and Ulke-Lemée, A. (2007). Emerging roles of nuclear protein phosphatases. *Nat. Rev. Mol. Cell Biol.* **8**, 234-244.
Oktem, O. and Urman, B. (2010). Understanding follicle growth in vivo. *Hum. Reprod.* **25**, 2944-2954.
Qi, S.-T., Wang, Z.-B., Ouyang, Y.-C., Zhang, Q.-H., Hu, M.-W., Huang, X., Ge, Z., Guo, L., Wang, Y.-P., Hou, Y. et al. (2013). Overexpression of SETbeta, a protein localizing to centromeres, causes precocious separation of chromatids during the first meiosis of mouse oocytes. *J. Cell Sci.* **126**, 1595-1603.
Qiao, J., Wang, Z.-B., Feng, H.-L., Miao, Y.-L., Wang, Q., Yu, Y., Wei, Y.-C., Yan, J., Wang, W.-H., Shen, W. et al. (2014). The root of reduced fertility in aged women and possible therapentic options: current status and future perspects. *Mol. Aspects Med.* **38**, 54-85.
Ruediger, R., Ruiz, J. and Walter, G. (2011). Human cancer-associated mutations in the Aalpha subunit of protein phosphatase 2A increase lung cancer incidence in Aalpha knock-in and knockout mice. *Mol. Cell. Biol.* **31**, 3832-3844.
Saskova, A., Solc, P., Baran, V., Kubelka, M., Schultz, R. M. and Motlik, J. (2008). Aurora kinase A controls meiosis I progression in mouse oocytes. *Cell Cycle* **7**, 2368-2376.
Schindler, K. (2011). Protein kinases and protein phosphatases that regulate meiotic maturation in mouse oocytes. *Results Probl. Cell Differ.* **53**, 309-341.
Stefansson, B. and Brautigan, D. L. (2006). Protein phosphatase 6 subunit with conserved Sit4-associated protein domain targets IkappaBepsilon. *J. Biol. Chem.* **281**, 22624-22634.
Stefansson, B. and Brautigan, D. L. (2007). Protein phosphatase PP6 N terminal domain restricts G1 to S phase progression in human cancer cells. *Cell Cycle* **6**, 1386-1392.
Stefansson, B., Ohama, T., Daugherty, A. E. and Brautigan, D. L. (2008). Protein phosphatase 6 regulatory subunits composed of ankyrin repeat domains. *Biochemistry* **47**, 1442-1451.
Sumiyoshi, E., Sugimoto, A. and Yamamoto, M. (2002). Protein phosphatase 4 is required for centrosome maturation in mitosis and sperm meiosis in C. elegans. *J. Cell Sci.* **115**, 1403-1410.
Sun, Q.-Y., Liu, K. and Kikuchi, K. (2008). Oocyte-specific knockout: a novel in vivo approach for studying gene functions during folliculogenesis, oocyte maturation, fertilization, and embryogenesis. *Biol. Reprod.* **79**, 1014-1020.
Sun, Q.-Y., Miao, Y.-L. and Schatten, H. (2009). Towards a new understanding on the regulation of mammalian oocyte meiosis resumption. *Cell Cycle* **8**, 2741-2747.
Sutton, A., Immanuel, D. and Arndt, K. T. (1991). The SIT4 protein phosphatase functions in late G1 for progression into S phase. *Mol. Cell. Biol.* **11**, 2133-2148.
Swain, J. E., Ding, J., Wu, J. and Smith, G. D. (2008). Regulation of spindle and chromatin dynamics during early and late stages of oocyte maturation by aurora kinases. *Mol. Hum. Reprod.* **14**, 291-299.
Tsai, M.-Y., Wiese, C., Cao, K., Martin, O., Donovan, P., Ruderman, J., Prigent, C. and Zheng, Y. (2003). A Ran signalling pathway mediated by the mitotic kinase Aurora A in spindle assembly. *Nat. Cell Biol.* **5**, 242-248.
Wang, Z.-B., Schatten, H. and Sun, Q.-Y. (2011). Why is chromosome segregation error in oocytes increased with maternal aging? *Physiology* **26**, 314-325.
Wang, Z.-B., Jiang, Z.-Z., Zhang, Q.-H., Hu, M.-W., Huang, L., Ou, X.-H., Guo, L., Ouyang, Y.-C., Hou, Y., Brakebusch, C. et al. (2013). Specific deletion of Cdc42 does not affect meiotic spindle organization/migration and homologous chromosome segregation but disrupts polarity establishment and cytokinesis in mouse oocytes. *Mol. Biol. Cell* **24**, 3832-3841.
Wassmann, K. (2013). Sister chromatid segregation in meiosis II: deprotection through phosphorylation. *Cell Cycle* **12**, 1352-1359.
Yao, L.-J., Zhong, Z.-S., Zhang, L.-S., Chen, D.-Y., Schatten, H. and Sun, Q.-Y. (2004). Aurora-A is a critical regulator of microtubule assembly and nuclear activity in mouse oocytes, fertilized eggs, and early embryos. *Biol. Reprod.* **70**, 1392-1399.
Zeng, K., Bastos, R. N., Barr, F. A. and Gruneberg, U. (2010). Protein phosphatase 6 regulates mitotic spindle formation by controlling the T-loop phosphorylation state of Aurora A bound to its activator TPX2. *J. Cell Biol.* **191**, 1315-1332.
Zhong, J., Liao, J., Liu, X., Wang, P., Liu, J., Hou, W., Zhu, B., Yao, L., Wang, J., Li, J. et al. (2011). Protein phosphatase PP6 is required for homology-directed repair of DNA double-strand breaks. *Cell Cycle* **10**, 1411-1419.